

1 Introduction

Text-to-CAD, the task of generating computer-aided design (CAD) models from natural-language descriptions, is emerging as a promising direction for AI-assisted 3D modeling [1]. Unlike Text-to-3D generation [2, 3], which typically uses mesh representations and emphasizes visual appearance, Text-to-CAD targets **design instances** that must satisfy practical requirements such as *functionality, manufacturability, and assemblability*. This shifts the focus from visual plausibility to engineering usability: the generated design must be geometrically valid and support downstream fabrication and assembly.

In recent years, Text-to-CAD datasets [1] have grown substantially. The existing datasets are built from modeling histories, such as command sequences and scripts, as summarized in Table 1. However, most existing datasets focus on single-part CAD models rather than complete design instances. As a result, they rarely capture multi-component structures or assembly constraints, and provide limited coverage of real-world use and fabrication requirements. Unlike standalone CAD parts, a dataset of design instances considering functionality, manufacturability, and assemblability is costly to build because each design instance requires a designer with extensive experience to expend a tremendous amount of effort. This makes every design instance extremely rare and highly valuable.

Beyond dataset construction, evaluation is another key challenge for Text-to-CAD. Most evaluations rely on geometric similarity metrics, such as Chamfer Distance (CD) [4], which measure visual resemblance to a reference shape but cannot reliably judge whether a generated model is a good design instance. For example, a chair that differs visually from the reference may still satisfy the same seating function, whereas a reference-like chair may still fail as a design if it is unstable, difficult to manufacture, or hard to assemble [5]. This highlights the need for Text-to-CAD evaluation protocols that assess design quality rather than geometric similarity alone.

To this end, we propose MUSE, a benchmark for functional, manufacturable, and assemblable Text-to-CAD generation. MUSE is constructed by the collaboration of human designers and LLM, focusing on practical CAD design instances rather than single-part CAD models. Each design instance is defined by a structured *Design Specification*, which decomposes a high-level design goal into physical assembly graph, valid parameter ranges and a manufacturing plan. Furthermore, to support engineering-grounded evaluation, each design instance is paired with program-generated CAD drawings for visual review. All design instances are carefully reviewed by human designers.

MUSE further introduces a three-stage evaluation protocol. First, we evaluate the executability of the *CadQuery* script generated by the latest LLMs and export the resulting CAD model. Second, we check the geometric validity of the exported CAD model, including watertightness, self-intersection, non-manifold features, and overlapping components. Third, we assess design-intent alignment using design-specific rubrics generated from the Design Specification, reference CAD drawings, reference code, and engineering knowledge tables. These rubrics characterize design validity in terms of functionality, manufacturability, and assemblability under the intended requirements.

Experiments on MUSE show that **current LLMs for Text-to-CAD remain far from producing usable designs**. Across both closed-source and open-source models, performance degrades sharply from code executability to geometric validity and then to design-intent alignment, revealing a clear failure cascade in practical CAD generation. Although closed-source models consistently outperform open-source ones, even the strongest model achieves only limited success on fine-grained criteria of functionality, manufacturability, and assemblability. We further show that our rubric-based visual language model (VLM) judge aligns well with human annotations, supporting scalable and reliable automatic evaluation.

2 Related Work

Text-to-CAD. Text-to-CAD aims to translate natural language into editable CAD models. Existing methods mainly follow two paradigms: *command-sequence generation*, which predicts low-level CAD operations such as extrusion or lofting [6–8, 4, 9], and *code-based generation*, which produces executable scripts such as *CadQuery* programs [4, 9]. Most existing datasets are derived from CAD construction sequences paired with synthetic or LLM-generated text [6, 7, 9, 4, 8], including DeepCAD [6], Text2CAD [7], and CADFusion [4].

However, current benchmarks largely focus on single-part or simple geometries and evaluate outputs using geometric metrics such as chamfer distance, parameter accuracy, or visual similarity [7, 4]. These metrics capture shape resemblance, but not whether a model is executable, geometrically valid as a B-Rep, or aligned with design intent. Recent work has begun to explore assembly-aware generation, e.g., ArtiCAD [10], but realistic assembly-level benchmarks and engineering-oriented evaluation remain limited. In contrast, MUSE focuses on complex, editable B-Rep assemblies paired with structured Design Specifications, and evaluates outputs by executability, geometric validity, and design-intent alignment, including functionality, manufacturability, and assemblability.

VLM-as-Judge. Vision-language models are increasingly used as automatic evaluators, but direct holistic scoring is often unstable and prone to multimodal hallucination [11–13]. Recent work therefore advocates fine-grained, factorized criteria [14–19]. This is especially important for CAD, where visually plausible outputs may still contain invalid geometry, incorrect interfaces, unstable structures, or infeasible manufacturing details [20–22].

Prior Text-to-CAD systems often use rendered views for feedback or evaluation [23, 24], and recent methods incorporate VLMs for CAD verification or refinement, such as CADCodeVerify [25], CADSmith [22], and EvoCAD [26]. However, rendered images can obscure CAD-specific failures due to perspective distortion, occlusion, and limited view coverage. Our evaluation instead targets *engineering correctness* through design-specific rubrics grounded in Design Specifications, reference engineering drawings, reference code, and engineering knowledge tables. Based on this formulation, we develop a rubric-based VLM judge for design-intent alignment and validate it against human annotation.

3 MUSE Benchmark

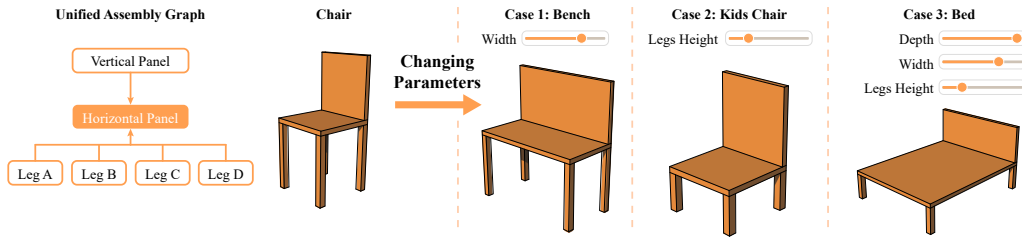


Figure 2: A unified assembly graph can correspond to different designs under different parameter settings, motivating the need for a valid parameter space Ω .

3.1 Preliminary: Defining Textual Inputs

Table 1: Comparison of textual inputs for Text-to-CAD tasks.

Input Type	Method	Textual Input Example	Tokens	Assemblable
CAD modeling Seq.	CADPrompt [27]; Pointer-CAD [28]; Text2CAD [1]	Sketch a large rectangle whose height is about 2/3rd its width. Create a square cutout from the rectangle, then extrude the remaining shape into the final 3D object.	80–120	No
High-level Design Desc.	CADFusion [29]	A rectangular prism with five square holes: one centrally located and four surrounding it.	20–40	No
	ArtiCAD [10]	Round table with four tapered legs: a circular tabletop and four tapered cylindrical supports.	40–60	Yes
Design Spec.	MUSE	A structured specification covering design goal, dimensions, material/process, joint type, parameter ranges, component roles, and textual Component Assembly Graph.	2500+	Yes

As mentioned in Section 1, existing textual inputs for Text-to-CAD (Table 1) mainly evaluate modeling-command following, rather than the ability to generate valid CAD models that satisfy

design intent. To evaluate the validation of CAD models, this study proposes a systematic, top-down *Design Specification* \mathcal{S} , which consists of design description [10], valid parameter space, a manufacturing plan, and an assembly plan, as shown in Figure 3:

$$\mathcal{S} = \langle \mathcal{D}, \mathcal{G}, \Omega, \mathcal{M} \rangle. \quad (1)$$

Definition 1 (Physical Assembly Graph). *A Physical Assembly Graph $\mathcal{G} = (\mathcal{V}, \mathcal{E})$ is an undirected graph, where each vertex $v_i \in \mathcal{V}$ denotes an individual physical component, such as a “seat panel” or a “support leg”, and each edge $e_{ij} \in \mathcal{E} \subseteq \mathcal{V} \times \mathcal{V}$ denotes a physical interface between components v_i and v_j .*

Given a target assembly graph \mathcal{G} , let $\Phi : \mathbb{C} \rightarrow \mathbb{G}$ map a CAD model C to its underlying assembly graph. A CAD model C is topologically valid with respect to \mathcal{G} if

$$\Phi(C) \cong \mathcal{G}, \quad (2)$$

where \cong denotes graph isomorphism. Models satisfying this condition are topologically equivalent with respect to \mathcal{G} . However, topological equivalence does not necessarily preserve design semantics. As illustrated in Figure 3, topologically equivalent designs may represent a chair, bench, kids chair, or bed by varying continuous parameters. Therefore, preserving the intended design semantics requires constraining these parameters within a valid parameter space.

Definition 2 (Valid Parameter Space). *Given a Physical Assembly Graph $\mathcal{G} = (\mathcal{V}, \mathcal{E})$, each component vertex $v_i \in \mathcal{V}$ is associated with a set of parameters \mathbf{p}_i , such as width, height, and thickness. The **Valid Parameter Space** Ω defines the admissible ranges of these parameters, as specified by the design description, functional requirements, and manufacturing constraints. A generated CAD model C is semantically valid only if the parameters of every component lie within their corresponding valid ranges.*

Definition 3 (Manufacturing Plan). *A set of Manufacturing Methods \mathcal{M} ensures that the generated CAD model remains compatible with real-world manufacturing constraints. It includes **material selections** (see Appendix 5), such as strength, brittleness, minimum thickness, and load-bearing capacity, and **manufacture methods** (see Appendix 6), such as minimum wall thickness in 3D printing and sheet-thickness limits in laser cutting. These constraints determine feasible ranges for component parameters, thereby shaping the valid parameter space Ω .*

3.2 Dataset Construction Pipeline

We introduce a dataset of strictly functional, manufacturable and assemblable CAD models. We employ a “Human-in-the-loop” pipeline that synergizes expert domain knowledge with LLM-driven scalable augmentation. The dataset curation pipeline consists of four stages, as illustrated in Figure 3.1. We first create high-quality seed 3D models with expert designers, then expand them into diverse 3D model variants using LLM-assisted CAD script augmentation. The resulting models are converted into standardized engineering views, and finally paired with structured Design Specifications.

Step 1: Expert-Driven Seed Models Construction. We first collect the design description and rendered reference examples of established designs across diverse design categories (e.g., chairs, tables, and business card holders). Following these instructions, professional designers manually construct high-quality 3D models in STEP format as the seed models. We then convert the designers’ modeling procedures into executable *CadQuery* scripts, which serve as the basis for subsequent augmentation.

Step 2: LLM-Powered Data Augmentation. To maximize dataset diversity, we use Claude Opus 4.7 to systematically expand the initial *CadQuery* scripts along two primary dimensions: *stylistic transformations* (e.g., adapting a traditional wooden chair into modern industrial aesthetics) and *functional repurposing* (e.g., evolving a chair’s into a shoe rack or coat stand).

Step 3: Engineering View Generation. To support reliable evaluation, we generate engineering views for all 3D models synthesized in the previous steps. Conventional rendered images [28] are less suitable for CAD assessment because they suffer from *perspective distortion*, *occlusion of internal structures*, and *incomplete spatial coverage*. To address these limitations, we leverage the underlying geometry kernel to explicitly extract precise boundaries, contours, and hidden lines from each 3D model, with hidden lines rendered as dashed paths. These geometric features are then normalized onto a unified 2×2 grid (Top, Front, Right, and Isometric views) within a standard vector canvas as

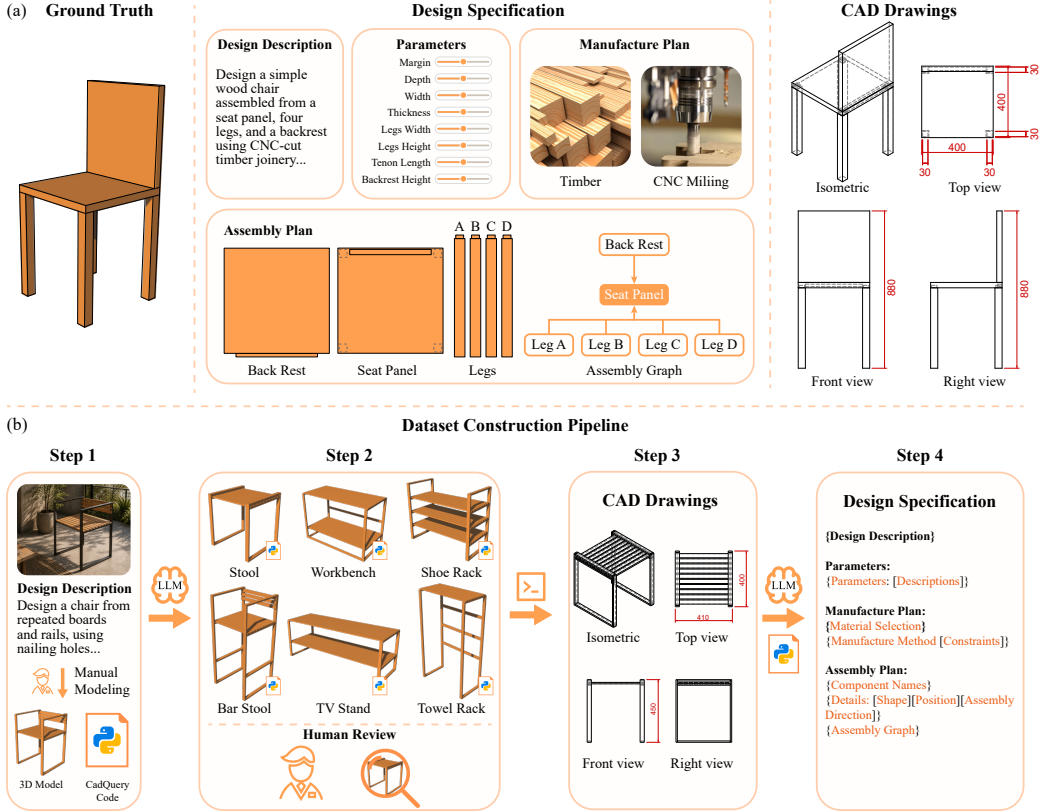


Figure 3: Overview of our dataset construction. (a) Each benchmark instance provides a Design Specification and standardized CAD drawings. (b) The dataset is curated through expert seed modeling, LLM-based augmentation, CAD drawing generation, and Design Specification synthesis.

is shown in Figure 3.1 (a). The resulting engineering views provide consistent visual evidence of component boundaries, hidden structures, and spatial relationships for downstream evaluation.

Step 4: Human-LLM Collaborative Design Specification Creation. Using the generated engineering views and *CadQuery* scripts, we employ few-shot prompting to synthesize structured Design Specifications \mathcal{S} . We manually construct several expert-written specifications as reference examples (see Appendix B). Conditioned on these examples, GPT-5.5 generates standardized specifications covering the design description \mathcal{D} , physical assembly graph \mathcal{G} , valid parameter space Ω , and manufacturing constraints \mathcal{M} . To ensure dataset quality, all synthesized \mathcal{D} are further reviewed and corrected by human experts.

3.3 Evaluation Protocol

We evaluate generated CAD models using the Design Specifications introduced in Section 3.2. Given a Design Specification \mathcal{S} , each Text-to-CAD model is prompted to generate a *CadQuery* script; the full prompt is provided in Appendix B. The generated script is then evaluated with a three-stage pipeline. As shown in Figure 4, an output must first pass code execution and geometric validation before it is assessed for design-intent alignment.

Three-stage Evaluation Protocol. Our evaluation proceeds in three stages. **Stage 1: Code Validity.** We execute the generated *CadQuery* script in a sandboxed environment and check whether it successfully constructs a CAD model and exports a STEP file. **Stage 2: Geometric Validity.** We then evaluate the exported STEP file using four binary geometry checks, illustrated in Figure 4. **Watertight** verifies that each solid is closed, with no open boundaries or naked edges. **Manifold** verifies that each solid has valid manifold topology. **Self-Intersection Free** verifies that each solid

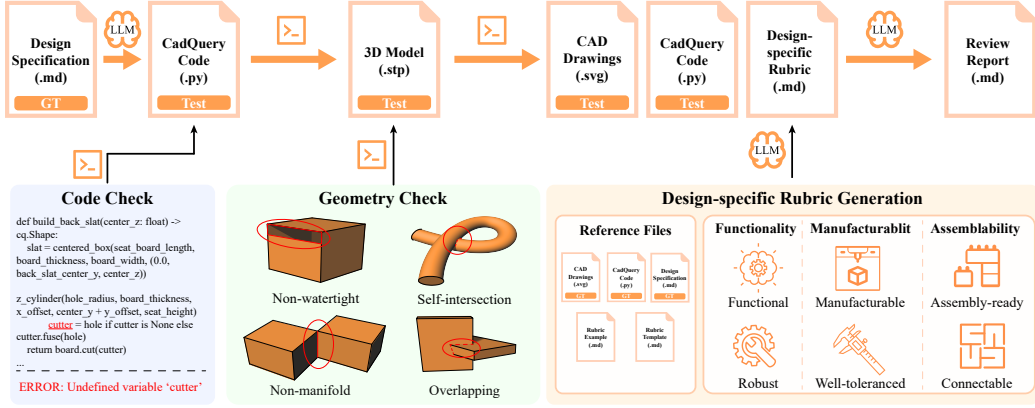


Figure 4: Illustration of the proposed evaluation system and rubric generation process. Given a Design Specification, each evaluated model generates a *CadQuery* script, which is executed and exported as a STEP file. After code and geometry validity checks, valid models are converted into standardized CAD drawings and assessed by a VLM judge using a design-specific rubric.

contains no self-intersecting faces or invalid internal overlaps. **Overlap Free** verifies that distinct solid components do not physically interpenetrate. Each check receives a score of 1 if satisfied and 0 otherwise. **Stage 3: Design-Intent Alignment.** Only STEP files that pass all geometric checks proceed to the final stage. We convert these valid outputs into engineering views and compare them with reference engineering views using a VLM judge under a design-specific rubric. Providing reference views gives the judge concrete visual evidence of the target structure and helps reduce hallucinated judgments. As summarized in Table 8, this stage evaluates three aspects: **functionality**, which checks whether the generated design remains valid over the parameter space Ω ; **manufacturability**, which checks whether the geometry satisfies the material and process constraints defined by \mathcal{M} ; and **assemblability**, which checks whether the component topology and interfaces specified by the assembly graph \mathcal{G} are preserved. The construction of the design-specific rubric is described next.

Evaluation Rubric Generation. Rather than judging generated CAD models by surface-level visual similarity, we construct a **design-specific rubric** for each task. This is necessary because different CAD objects demand different engineering priorities: for example, a chair emphasizes load-bearing capacity and stability, whereas a vase emphasizes containment. The rubric generator takes as input the Design Specification \mathcal{S} , reference engineering views, the reference *CadQuery* script, expert examples, and a general rubric template; the full prompt is provided in Appendix B.

We produce six binary sub-criteria, whose construction logic is summarized in Table 8. *Assembly-ready* asks the judge to infer the component graph from the generated views and compare it with the target graph. *Connectable* extracts the required joint type and verifies the joint location, assembly direction, and joint behavior. *Well-toleranced* identifies the relevant manufacturing process, retrieves the corresponding tolerance requirements, and uses the reference views as visual scale. *Functional* extracts the required functions from the design goal and specifies the structures needed to support them. *Robust* infers the expected support behavior and force-transfer path from component topology and joint relations. *Manufacturable* extracts the material and manufacturing process, retrieves the corresponding material-process constraints, and checks for geometries that violate them.

4 Experiments

In this section, we first present an overview of the proposed MUSE benchmark. We then evaluate both closed-source and open-source LLMs using our three-stage evaluation pipeline. Finally, we assess the reliability of the VLM-based judge through human annotation.

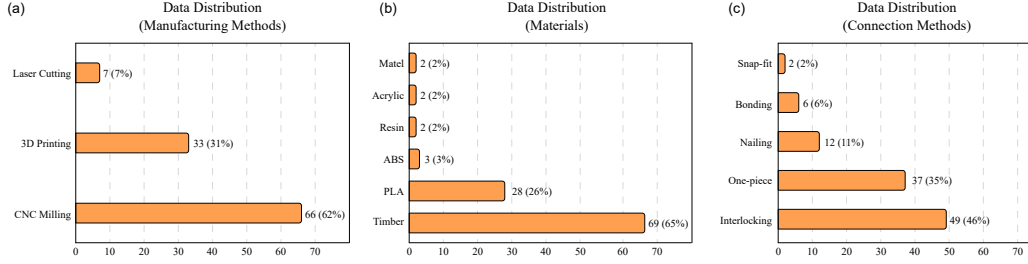


Figure 5: Dataset statistics of MUSE, showing the distributions of (a) manufacturing methods, (b) materials, and (c) connection methods across all design instances.

4.1 Data Distribution of MUSE

MUSE comprises 106 design instances spanning a wide range of manufacturing processes, materials, and connection methods, as summarized in Figure 5. The benchmark includes representative manufacturing processes such as computer numerical control (CNC) milling, 3D printing, and laser cutting, with CNC milling constituting the largest category. In terms of material usage, timber and polylactic acid filaments (PLA) are the most prevalent. Regarding connection methods, one-piece designs represent single-body objects, whereas interlocking, nailing, and snap-fit designs correspond to multi-component assemblies. Overall, these distributions indicate that MUSE places particular emphasis on assemblable CAD models while maintaining broad coverage of real-world manufacturable design scenarios.

Table 2: Per-model results across the three evaluation stages, judged by *Gemini-3.1-Pro*. The table reports code execution, geometric validity, and design-intent alignment scores under our funnel-style evaluation protocol. Bold marks the best score per block.

Model	Code Check (%)		Geometry Check (%)				Design Intent Alignment (%)			Final Score
	Sandbox Success	Watertight	Manifold	Self-Int. Free	Overlap Free	Geom. Valid	Functionality	Manufacturability	Assemblability	
<i>Closed-Source Models</i>										
claude-opus-4.7	76.42	76.42	76.42	73.58	60.38	58.49	42.92	36.79	38.68	39.47
claude-3.7-sonnet	46.23	46.23	46.23	46.23	23.58	23.58	12.26	11.79	14.15	12.74
gemini-3.1-pro	65.09	59.43	63.21	63.21	62.26	58.49	47.64	41.04	41.51	43.40
glm-5.1	31.13	31.13	31.13	31.13	27.36	27.36	18.87	17.45	20.28	18.87
glm-4.7-flash	8.49	7.55	7.55	7.55	5.66	5.66	1.89	2.36	2.83	2.36
gpt-5.5	77.36	72.64	74.53	73.58	70.75	68.87	54.72	48.58	53.77	52.36
gpt-4o	36.79	36.79	36.79	36.79	13.21	13.21	3.77	4.72	6.60	5.03
minimax-m2.7	18.87	18.87	18.87	18.87	10.38	10.38	5.19	5.66	6.13	5.66
minimax-m2.5	25.47	22.64	22.64	22.64	10.38	10.38	1.89	2.83	3.77	2.83
Average	42.87	41.30	41.93	41.51	31.55	30.71	21.02	19.03	20.86	20.30
<i>Open-Source Models</i>										
qwen-3.5-122b-a10b	27.36	25.47	25.47	25.47	13.21	13.21	8.49	7.55	8.96	8.33
qwen-2.5-72b	50.00	49.06	49.06	49.06	19.81	20.75	2.83	4.72	5.66	4.40
llama-3.1-70b	31.13	30.19	30.19	30.19	22.64	23.58	0.94	2.83	2.83	2.20
qwen-3.6-35b-a3b	8.49	8.49	8.49	8.49	5.66	5.66	3.77	3.77	4.72	4.09
qwen-3.6-coder	14.15	14.15	14.15	14.15	10.38	10.38	3.77	3.30	2.83	3.30
llama-3.1-8b	2.83	1.89	1.89	1.89	0.94	1.89	0.00	0.00	0.00	0.00
Average	22.33	21.54	21.54	21.54	12.11	12.58	3.30	3.69	4.17	3.72

4.2 Evaluation of Closed-Source and Open-Source LLMs

We evaluate a broad set of closed-source and open-source LLMs using the proposed three-stage evaluation pipeline. Given a Design Specification \mathcal{S} , each model is prompted to generate a *CadQuery* script, which is then assessed for (1) code validity, (2) geometric validity, and (3) alignment with the design intent. These three stages form a funnel-style evaluation: samples that fail at an earlier stage receive a score of zero for all subsequent metrics. The closed-source models evaluated include GPT-5.5, GPT-4o, Claude Opus 4.7, Claude 3.7 Sonnet, Gemini 3.1 Pro, GLM-5.1, GLM-4.7-

Table 3: Stage 3 sub-criterion breakdown judged by *Gemini-3.1-Pro*; *Average* is the mean of the two sub-criterion columns to its left. Bold marks the best score per block.

Model	Functionality (%)			Manufacturability (%)			Assemblability (%)		
	Functional	Robust	Average	Well-toleranced	Manufacturable	Average	Assembly-ready	Connectable	Average
<i>Closed-Source Models</i>									
claude-opus-4.7	43.40	42.45	42.92	33.02	40.57	36.79	43.40	33.96	38.68
claude-3.7-sonnet	11.32	13.21	12.26	11.32	12.26	11.79	14.15	14.15	14.15
gemini-3.1-pro	48.11	47.17	47.64	41.51	40.57	41.04	43.40	39.62	41.51
glm-5.1	17.92	19.81	18.87	16.04	18.87	17.45	21.70	18.87	20.28
glm-4.7-flash	1.89	1.89	1.89	1.89	2.83	2.36	2.83	2.83	2.83
gpt-5.5	54.72	54.72	54.72	49.06	48.11	48.58	55.66	51.89	53.77
gpt-4o	1.89	5.66	3.77	3.77	5.66	4.72	6.60	6.60	6.60
minimax-m2.7	5.66	4.72	5.19	5.66	5.66	5.66	6.60	5.66	6.13
minimax-m2.5	1.89	1.89	1.89	1.89	3.77	2.83	4.72	2.83	3.77
<i>Average</i>	20.75	21.28	21.02	18.24	19.81	19.03	22.12	19.60	20.86
<i>Open-Source Models</i>									
qwen-3.5-122b-a10b	7.55	9.43	8.49	6.60	8.49	7.55	8.49	9.43	8.96
qwen-2.5-72b	1.89	3.77	2.83	2.83	6.60	4.72	6.60	4.72	5.66
llama-3.1-70b	0.00	1.89	0.94	1.89	3.77	2.83	2.83	2.83	2.83
qwen-3.6-35b-a3b	2.83	4.72	3.77	2.83	4.72	3.77	5.66	3.77	4.72
qwen-3.6-coder	2.83	4.72	3.77	2.83	3.77	3.30	2.83	2.83	2.83
llama-3.1-8b	0.00	0.00	0.00	0.00	0.00	0.00	0.00	0.00	0.00
<i>Average</i>	2.52	4.09	3.30	2.83	4.56	3.69	4.40	3.93	4.17

Flash, MiniMax-M2.7, and MiniMax-M2.5. The open-source models include Qwen3.5-122B-A10B, Qwen2.5-72B, Llama-3.1-70B, Qwen3.6-35B-A3B, Qwen3.6-Coder, and Llama-3.1-8B.

Inapplicability of Existing Text-to-CAD Baselines. We do not directly evaluate existing Text-to-CAD methods, as their task settings differ fundamentally from ours and are not applicable to our benchmark. Prior work primarily uses command-sequence-style inputs to generate isolated primitive or single-part CAD models [30–32, 25, 28]. These methods are architecturally and procedurally tailored to such data and interaction paradigms, and thus cannot be directly applied to our design instances, which are manufacturable multi-component assemblies with explicit component relations and manufacturing constraints. ArtiCAD [10], posted on arXiv in mid-April, is the only assembly-level baseline, but its code is not publicly available, so we cannot evaluate it on our benchmark.

4.3 Experimental Results and Analysis

Tables 2 and 3 summarize results under our three-stage evaluation pipeline. Table 2 reports performance from code execution, to geometric validity, to design-intent alignment. The pipeline is strictly sequential: a sample advances only if it passes all checks in the previous stage; otherwise, it receives a score of 0 for all downstream metrics. In the Geometry Check stage, *Geom. Valid* denotes the fraction of samples that pass all geometric checks. In the final stage, *Final Score* is the mean of functionality, manufacturability, and assemblability after all three stages. Table 3 further decomposes these three pillars into six rubric-level criteria.

RQ1: What are the main bottlenecks for LLMs in practical Text-to-CAD generation? Table 2 reveals a clear failure cascade. First, generating an executable *CadQuery* script is already difficult. Second, among geometric checks, *Overlap Free* drops much more sharply than *Watertight*, *Manifold*, and *Self-Int. Free*, indicating that multi-component spatial reasoning is a major bottleneck even when the code executes. Third, Design Intent Alignment causes another substantial drop, showing that geometric validity does not translate to functional, manufacturable, or assemblable designs. The core challenge is therefore not just code synthesis, but coherent assembly generation under coupled geometric and engineering constraints.

RQ2: How do closed-source and open-source models differ in Text-to-CAD generation? Closed-source models outperform open-source models across all stages, with GPT-5.5 achieving the strongest overall performance. The gap is not limited to code execution. Claude Opus 4.7, for example, attains

Table 4: Correlation between LLM judges and human annotators on the SVG benchmark (20 design instances; $n = 624$ sub-criteria, 312 criteria, 104 design instances).

Level	Gemini 3.1 Pro			GPT-5.5			GPT-4o		
	Pearson r	Spearman ρ	Kendall τ	Pearson r	Spearman ρ	Kendall τ	Pearson r	Spearman ρ	Kendall τ
Sub-criteria	0.713	0.705	0.655	0.659	0.653	0.607	0.620	0.609	0.566
Criteria	0.762	0.749	0.668	0.712	0.705	0.626	0.703	0.685	0.610
Design instance	0.835	0.831	0.694	0.775	0.773	0.654	0.826	0.799	0.663

a relatively high execution rate but drops substantially in *Geom. Valid*, showing that executable code often still produces invalid assemblies. Open-source models underperform both upstream and downstream: even at similar execution rates, they tend to lose more samples in Geometry Check and Design Intent Alignment. This indicates weaker control over both geometric consistency and engineering intent.

RQ3: How well do models satisfy fine-grained design criteria? Table 3 shows that fine-grained design criteria remain difficult across all three pillars. Even the best closed-source models achieve only about 19–21% on functionality, manufacturability, and assemblability, while open-source models remain around 3–4%. Passing code and geometry checks is therefore far from sufficient for practical Text-to-CAD generation. Current models still struggle to produce assemblies that satisfy real design requirements.

RQ4: Does stronger code generation imply stronger CAD geometry generation? Table 2 shows that code executability does not necessarily translate into better CAD generation. For example, qwen-2.5-72b achieves the highest open-source execution rate, but its *Geom. Valid* and Design Intent Alignment scores remain low. In contrast, llama-3.1-70b has a lower execution rate but achieves better geometric validity. This suggests that code-oriented capability alone is insufficient for Text-to-CAD, which also requires 3D spatial reasoning and design-intent understanding.

4.4 Human Alignment of the VLM Judge

To assess the reliability of our VLM-based judge, we randomly sample 20 design instances and ask four annotators (across two annotation rounds) to independently score each rendered SVG on six binary rubric sub-criteria. The final human label is the mean of the available annotations per cell. We measure judge–human agreement at three granularities: *sub-criteria* ($n = 624$), *criteria* ($n = 312$), obtained by averaging each pair of sub-criteria into one criterion, and *design instance* ($n = 104$), obtained by averaging all six sub-criteria.

As shown in Table 4, Gemini 3.1 Pro achieves the strongest agreement with human annotation at the sub-criteria level (Pearson $r = 0.713$), followed by GPT-5.5 ($r = 0.659$) and GPT-4o ($r = 0.620$); corresponding 95% bootstrap confidence intervals are reported in Table 11. Relative to prior LLM-as-judge results, our strongest sub-criteria-level correlation (0.713) is comparable to FLASK [33] (0.673 and 0.732), and exceeds the GPT-4 Spearman correlation reported in G-Eval [34] (0.514). At the design-instance level, agreement reaches $r \approx 0.83$ for the two best judges, approaching the 85% GPT-4–human pairwise agreement reported by MT-Bench [35]. Overall, these results indicate that the SVG-based judge is well aligned with human annotation at both fine-grained and instance levels, supporting its use for automatic evaluation.

5 Conclusion

We introduced MUSE, a benchmark that recasts Text-to-CAD as an engineering-grounded generation problem, with evaluation spanning executability, geometric validity, and design-intent alignment. Unlike prior benchmarks centered on modeling histories or geometric resemblance, MUSE asks a harder and more practical question: *can existing LLMs generate a design that actually works?*

Our results suggest that, today, the answer is largely no. Current LLMs can sometimes produce executable scripts and superficially plausible geometry, but they still fail to reliably satisfy functional, manufacturing, and assembly requirements. This exposes a core weakness of the field: Text-to-CAD has been easier to measure as shape generation than to solve as design generation. By making that gap explicit, MUSE raises the bar from producing CAD that looks right to producing CAD that is

right. We hope this benchmark drives future work toward models that generate designs that can be built, assembled, and used in practice.

Limitations. MUSE has two current limitations. First, the CAD models in our benchmark have not been physically manufactured; instead, they are validated by professional designers, which may not capture all real-world manufacturing issues. Second, our evaluation does not yet model the full physical assembly process: the *Connectable* criterion checks geometric feasibility of joints but not assembly order, and the *Robust* criterion relies on LLM-based qualitative assessment rather than physics-based quantitative analysis. Future work includes extending the benchmark to more complex assemblies, incorporating physics-aware evaluation, and comparing with additional assembly-level baselines as their implementations become available.

References

- [1] Mohammad S Khan, Sankalp Sinha, Talha U Sheikh, Didier Stricker, Sk A Ali, and Muhammad Z Afzal. Text2CAD: generating sequential cad designs from beginner-to-expert level text prompts. *Advances in Neural Information Processing Systems*, 37:7552–7579, 2024.
- [2] Dmitry Tochilkin, David Pankratz, Zexiang Liu, Zixuan Huang, Adam Letts, Yangguang Li, Ding Liang, Christian Laforte, Varun Jampani, and Yan-Pei Cao. Triposr: fast 3d object reconstruction from a single image. *arXiv preprint arXiv:2403.02151*, 2024.
- [3] Dong-Yang Li, Yi-Long Liu, Zi-Xian Liu, Yan-Pei Cao, Meng-Hao Guo, and Shi-Min Hu. SeparateGen: semantic component-based 3D character generation from single images. *IEEE Transactions on Visualization and Computer Graphics*, 2026.
- [4] Ruiyu Wang, Yu Yuan, Shizhao Sun, and Jiang Bian. Text-to-CAD generation through infusing visual feedback in large language models. In *Proceedings of the International Conference on Machine Learning (ICML)*, 2025.
- [5] Jiaming Ma, Zhi Li, Zi-Long Zhao, and Yi Min Xie. Creating novel furniture through topology optimization and advanced manufacturing. *Rapid Prototyping Journal*, 27(9):1749–1758, 2021.
- [6] Rundi Wu, Chang Xiao, and Changxi Zheng. DeepCAD: A deep generative network for computer-aided design models. In *Proceedings of the IEEE/CVF International Conference on Computer Vision (ICCV)*, pages 6772–6782, October 2021.
- [7] Mohammad Sadil Khan, Sankalp Sinha, Talha Uddin Sheikh, Didier Stricker, Sk Aziz Ali, and Muhammad Zeshan Afzal. Text2CAD: generating sequential CAD models from beginner-to-expert level text prompts. In *Advances in Neural Information Processing Systems (NeurIPS)*, pages 7552–7579, 2024.
- [8] Siyu Wang, Cailian Chen, Xinyi Le, Qimin Xu, Lei Xu, Yanzhou Zhang, and Jie Yang. CAD-GPT: synthesising CAD construction sequence with spatial reasoning-enhanced multimodal LLMs. In *Proceedings of the AAAI Conference on Artificial Intelligence*, volume 39, pages 7880–7888, 2025.
- [9] Xueyang Li, Yu Song, Yunzhong Lou, and Xiangdong Zhou. CAD translator: an effective drive for text to 3D parametric computer-aided design generative modeling. In *Proceedings of the ACM International Conference on Multimedia (ACM MM 2024), Poster*, 2024.
- [10] Yuan Shui, Yandong Guan, Zhanwei Zhang, Juncheng Hu, Jing Zhang, Dong Xu, and Qian Yu. ArtiCAD: articulated CAD assembly design via multi-agent code generation. *arXiv preprint arXiv:2604.10992*, 2026.
- [11] Dongping Chen, Ruoxi Chen, Shilin Zhang, Yinuo Liu, Yaochen Wang, Huichi Zhou, Qihui Zhang, Yao Wan, Pan Zhou, and Lichao Sun. MLLM-as-a-Judge: Assessing multimodal LLM-as-a-judge with vision-language benchmark. In *International Conference on Machine Learning (ICML)*, 2024.
- [12] Wentao Ge, Shunian Chen, Guiming Hardy Chen, et al. MLLM-Bench: evaluating multimodal LLMs with per-sample criteria. *arXiv preprint arXiv:2311.13951*, 2024.

- [13] Md Tahmid Rahman Laskar, Mohammed Saidul Islam, Ridwan Mahbub, Ahmed Masry, Mizanur Rahman, Amran Bhuiyan, Mir Tafseer Nayeem, Shafiq Joty, Enamul Hoque, and Jimmy Huang. Judging the judges: Can large vision-language models fairly evaluate chart comprehension and reasoning? In *Proceedings of the 63rd Annual Meeting of the Association for Computational Linguistics (Volume 6: Industry Track)*, pages 1203–1216, 2025.
- [14] Seongyun Lee, Seungone Kim, Sue Park, Geewook Kim, and Minjoon Seo. Prometheus-vision: Vision-language model as a judge for fine-grained evaluation. In *Findings of the Association for Computational Linguistics: ACL 2024*, pages 11286–11315, 2024.
- [15] Runzhou Liu, Hailey Weingord, Sejal Mittal, et al. Human-Aligned MLLM judges for fine-grained image editing evaluation: a benchmark, framework, and analysis. *arXiv preprint arXiv:2602.13028*, 2026.
- [16] Yukang Feng, Jianwen Sun, Chuanhao Li, et al. A high-quality dataset and reliable evaluation for interleaved image-text generation. *arXiv preprint arXiv:2506.09427*, 2025.
- [17] Ruihang Li, Leigang Qu, Jingxu Zhang, Dongnan Gui, Mengde Xu, Xiaosong Zhang, Han Hu, Wenjie Wang, and Jiaqi Wang. Genarena: How can we achieve human-aligned evaluation for visual generation tasks? *arXiv preprint arXiv:2602.06013*, 2026.
- [18] Zhikai Li, Jiatong Li, Xuwen Liu, et al. K-Sort eval: efficient preference evaluation for visual generation via corrected VLM-as-a-Judge. In *International Conference on Learning Representations (ICLR)*, 2026.
- [19] Tianyi Xiong, Xiyao Wang, Dong Guo, Qinghao Ye, Haoqi Fan, Quanquan Gu, Heng Huang, and Chunyuan Li. Llava-critic: Learning to evaluate multimodal models. In *Proceedings of the Computer Vision and Pattern Recognition Conference*, pages 13618–13628, 2025.
- [20] Zeyu Chen, Huanjin Yao, Ziwang Zhao, and Min Yang. Advancing multimodal judge models through a capability-oriented benchmark and mcts-driven data generation. *arXiv preprint arXiv:2603.00546*, 2026.
- [21] Tianyi Xiong, Yi Ge, Ming Li, et al. Multi-Crit: Benchmarking multimodal judges on pluralistic criteria-following. *arXiv preprint arXiv:2511.21662*, 2025.
- [22] Jesse Barkley, Rumi Loghmani, and Amir Barati Farimani. Cadsmith: Multi-agent cad generation with programmatic geometric validation. *arXiv preprint arXiv:2603.26512*, 2026.
- [23] Ruiyu Wang, Yu Yuan, Shizhao Sun, and Jiang Bian. Text-to-cad generation through infusing visual feedback in large language models. *arXiv preprint arXiv:2501.19054*, 2025.
- [24] Hao Ji, Kotha Aditya, Sebastian Escalante, and Yunjian Qiu. Codegen-3d: A benchmark for evaluating llms in zero-shot and iterative 3d modeling in blender. *IEEE Access*, 2026.
- [25] Kamel Alrashedy, Pradyumna Tambwekar, Zulfiqar Zaidi, Megan Langwasser, Wei Xu, and Matthew Gombolay. Generating CAD code with vision-language models for 3D designs. *arXiv preprint arXiv:2410.05340*, 2024.
- [26] Tobias Preintner, Weixuan Yuan, Adrian König, Thomas Bäck, Elena Raponi, and Niki Van Stein. EvoCAD: evolutionary CAD code generation with vision language models. In *2025 IEEE 37th International Conference on Tools with Artificial Intelligence (ICTAI)*, pages 504–511. IEEE, 2025.
- [27] Kamel Alrashedy, Pradyumna Tambwekar, Zulfiqar Zaidi, Megan Langwasser, Wei Xu, and Matthew Gombolay. Generating CAD code with vision-language models for 3D designs. *arXiv preprint arXiv:2410.05340*, 2024.
- [28] Dacheng Qi, Chenyu Wang, Jingwei Xu, Tianzhe Chu, Zibo Zhao, Wen Liu, Wenrui Ding, Yi Ma, and Shenghua Gao. Pointer-CAD: unifying B-Rep and command sequences via pointer-based edges & faces selection. *arXiv preprint arXiv:2603.04337*, 2026.
- [29] Ruiyu Wang, Yu Yuan, Shizhao Sun, and Jiang Bian. Text-to-CAD generation through infusing visual feedback in large language models. *arXiv preprint arXiv:2501.19054*, 2025.

- [30] Jingwei Xu, Chenyu Wang, Zibo Zhao, Wen Liu, Yi Ma, and Shenghua Gao. CAD-MLLM: Unifying multimodality-conditioned CAD generation with MLLM. *arXiv preprint arXiv:2411.04954*, 2024.
- [31] Jianxing Liao, Junyan Xu, Yatao Sun, Maowen Tang, Sicheng He, Jingxian Liao, Shui Yu, Yun Li, and Xiaohong Guan. Automated CAD modeling sequence generation from text descriptions via transformer-based large language models. In *Proceedings of the 63rd Annual Meeting of the Association for Computational Linguistics (Volume 1: Long Papers)*, pages 21720–21748, 2025.
- [32] Mohsen Yavartanoo, Sangmin Hong, Reyhaneh Neshatavar, and Kyoung Mu Lee. Text2CAD: text to 3D CAD generation via technical drawings. *arXiv preprint arXiv:2411.06206*, 2024.
- [33] Seonghyeon Ye, Doyoung Kim, Sungdong Kim, Sahana Hwang, Seungone Kim, Yongrae Jo, James Thorne, Juho Kim, and Minjoon Seo. FLASK: Fine-grained language model evaluation based on alignment skill sets. In *ICLR*, 2024.
- [34] Yang Liu, Dan Iter, Yichong Xu, Shuohang Wang, Ruochen Xu, and Chenguang Zhu. G-Eval: NLG evaluation using GPT-4 with better human alignment. In *EMNLP*, 2023.
- [35] Lianmin Zheng, Wei-Lin Chiang, Ying Sheng, Siyuan Zhuang, Zhanghao Wu, Yonghao Zhuang, Zi Lin, Zhuohan Li, Dacheng Li, Eric P. Xing, Hao Zhang, Joseph E. Gonzalez, and Ion Stoica. Judging LLM-as-a-Judge with MT-Bench and chatbot arena. In *NeurIPS Datasets and Benchmarks Track*, 2023.

A Engineering Knowledge Tables for Manufacturability

To systematically evaluate the manufacturability of a design, it is essential to consider the interplay between materials, fabrication processes, and assembly techniques. This section outlines the foundational engineering guidelines required to optimize designs for real-world production. Table 5 presents a comprehensive overview of various materials, detailing their mechanical properties, process compatibility, and typical applications. Table 6 delineates the technical capabilities, geometric constraints, and cost implications of common manufacturing methods, highlighting the trade-offs between precision and production feasibility. Finally, Table 7 categorizes standard mechanical connection methods, illustrating how different joint types constrain degrees of freedom (DoF) during assembly. Together, these references establish a structured framework for design for manufacturability (DFM).

Table 5: Material Selection: Features and Typical Applications

Material	Compatible Processes	Features	Typical Applications
Timber	CNC, Laser Cutting	Easy to machine, medium strength, natural texture	Furniture, structural parts, DIY decor
ABS	3D Printing	High toughness, heat resistant	Structural components, enclosures
PLA	3D Printing	Easy to print, eco-friendly, low strength	Rapid prototypes, aesthetic models
TPU	3D Printing	Flexible, high elasticity	Seals, gaskets, cushioning parts
Acrylic	CNC, Laser Cutting	Transparent, rigid but brittle	Housings, lighting, displays
Resin	3D Printing	High precision, fine detail, brittle	Intricate models, dental, figurines
Sheet Metal	CNC, Laser Cutting	Lightweight, rapid forming	Chassis, enclosures
Aluminum	CNC Milling	High strength-to-weight ratio, corrosion resistant	Structural parts, high-end housings
Steel	CNC Milling	High strength and stiffness, heavy	Mechanical structures, supports

B Prompt Templates

This appendix provides the prompt templates used throughout our benchmark construction and evaluation pipeline. Specifically, the first prompt is used in the human-LLM collaborative dataset

Table 6: Technical Specifications and Constraints of Manufacturing Methods

Method	Constraints	Precision	Cost	Materials	Features	Diff.
CNC Milling	2.5D/3-axis limits, tool radius offsets, max edge < 2000 mm	±0.05-0.10 mm	Med-High	Wood, Al, Plastic	High precision; complex surfaces; restricted by tool paths	Low
Laser Cutting	2D only, thickness < 5 mm, max edge < 2000 mm	±0.05-0.20 mm	Low-Med	Wood, Acrylic, Metal	Fast; low cost; ideal for interlocking assembly structures	Low
3D Printing	Build volume within 300 × 300 × 300 mm	±0.10-0.50 mm	Low	PLA, ABS, TPU	High freedom; rough surface, anisotropic strength, visible layer lines	Low
Injection Molding	Requires molds and draft angles; must be demoldable	±0.01-0.05 mm	High	Plastics	High precision and consistency; best for mass production	High
Silicone Casting	Dependent on master mold; shrinkage and bubble risks	±0.1-0.3 mm	Low-Med	Resin, Silicone	Suitable for small batch replication; cheaper than injection	High
Modular Assembly	Dependent on standard part sizes; tolerance stack-up	±0.10-0.50 mm	Low	Standard Parts, Profiles	Rapid construction; requires no additional manufacturing	Low

construction stage to convert CAD assets into structured Design Specifications. The second prompt is used for design-specific evaluation, where a VLM generates task-specific rubrics for assessing design-intent alignment in terms of functionality, manufacturability, and assemblability.

System Prompt: CAD Design Specification Generator

System Prompt: CAD Design Specification Agent

Role

You are an Expert CAD Systems Engineer and Manufacturing Specialist. Your goal is to analyze provided CAD data (CadQuery code, SVG/STP files) and decompose it into a formal, engineering-grade **Design Specification** (Design Task Document) in **English**.

Core Task

Generate a structured document that defines the design intent, physical constraints, and manufacturing requirements of a 3D model based on its B-Rep logic and parametric script.

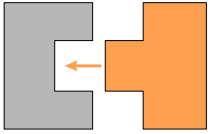
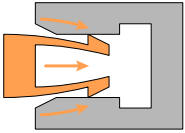
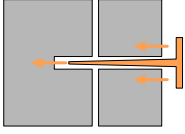
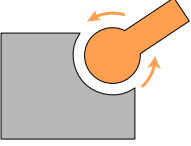
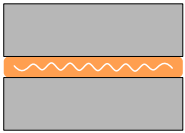
Constraints for Technical Selection

You **MUST** select the **Material**, **Manufacturing Method**, and **Connection Method** strictly from the provided technical tables in the 'Reference Tables' section below. Do not hallucinate external methods.

Inference Logic

- * **Analyze Joint Type:** Look at boolean operations in CadQuery ('cut', 'fuse', 'intersect'). If a component has a protruding box ('tenon') and another has a subtracted hole ('socket/mortise'), select **Mortise & Tenon**.
- * **Analyze Manufacturing:** Based on the geometry (e.g., 2.5D shapes are suitable for CNC/Laser, complex 3D shapes for Printing) and the selected material.
- * **Analyze Parameters:** Extract variable names and ranges from dictionaries like 'PARAM_RANGES' or script constants.

Table 7: Classification and Features of Connection Methods

Joint Type	Features	Illustration
Interlocking	Typically constrains all 6 DoF when properly fitted	
Snap-fit	Nearly fully constrained; relies on elastic deformation	
Nailing	Partially constrains motion; allows rotation and axial slip (depending on friction)	
Pivot	Constraints 5 DoF, allowing 1 rotational axis	
Bonding	Fully constrained in all directions (permanent)	

```

## Output Format Requirements
Your response MUST strictly follow the Markdown structure below:

# Design Specification

## Design Goal
[Concise description of what the object is and its primary function.]

## Geometry and Dimensions
Approx. [Width] mm × [Depth] mm × [Height] mm.

## Material
[Select strictly from Table 1]
    
```

Table 8: Evaluation criteria used in the design-intent alignment stage.

Criterion	Sub-criterion	Evaluation Question	Evidence Used
Functionality	Functional	Can the object support its intended primary use and auxiliary function?	Design Specification; functional requirements; visual proportions and structures in <Generated_SVG>.
	Robust	Can the object remain stable and structurally reliable during use?	Mechanical condition; component topology; joint relationships; support posture and load-transfer path in <Generated_SVG>.
Manufacturability	Manufacturable	Can the object be realistically fabricated under the specified material and manufacturing process?	Material; manufacturing method; material/process knowledge tables; geometric features in <Generated_SVG>.
	Well-toleranced	Are seams, clearances, wall thicknesses, and contact gaps consistent with the required process precision?	Manufacturing method; process tolerance table; <Reference_SVG> as visual scale; seams, clearances, and wall thicknesses in <Generated_SVG>.
Assemblability	Assembly-ready	Does the object preserve the intended component topology?	Component Assembly Graph in the Design Specification; visible components as graph nodes; physical connections as graph edges; <Generated_SVG>.
	Connectable	Are the physical joints placed, oriented, and constrained correctly?	Joint type; assembly direction; connection-method knowledge table; joint locations and contact regions in <Generated_SVG>.

```

## Manufacturing Method
[Select strictly from Table 2]

## Connection Method (Joint Type)
[Select strictly from Table 3]

## Mechanical Condition
[User scenario, e.g., Single-person seating, load-bearing storage, etc.]

## Structural Features
[List main components separated by semicolons; e.g., Seat panel; four legs;
backrest.]

## Special Requirements
[Any constraints like "Keep assembly split unchanged".]

## Planned Component Quantity
[Count of independent solid bodies]

## Component Names
- [Part Name 1]

```

```

- [Part Name 2]
...

## Adjustable Parameters
- **[Parameter Name]**: [Value] ([Min] ~ [Max] mm). [Reasoning/Constraint
  description].

## Component Details

### [Component Number]. [Component Name]
[Brief description of the part's role in the assembly.]
* **Component Purpose**: [Specific functional role].
* **Assembly Direction**: [Vector/Direction, e.g., Vertical insertion along
  +Z axis].
* **Connection & Kinematics**: [Joint Type from Table 3] ([Degrees of
  Freedom/Kinematics description from Table 3]).

---

## Component Assembly Graph (Textual)
[Part A] -> [Part B] | Joint: [Type] | Note: [Description of the interface]

---

## Reference Tables (Knowledge Base)
...

```

System Prompt: Vision-LLM Rubric Generator

Role and Objective

You are a top-tier expert in CAD (Computer-Aided Design), physical manufacturing, and assembly evaluation. Your task is to dynamically write a rigorous 0--1 Pass/Fail evaluation rubric for an AI-generated 3D model.

The rubric you generate will be injected into the '<Evaluation_Rubric>' placeholder and used by a downstream Vision-LLM judge to evaluate '<Generated_SVG>'.

Background Knowledge Base

When reasoning about tolerances, joint relationships, and manufacturability, you must cross-reference the following three tables.

Table 1: Manufacturing Methods

Method	Constraints	Precision / Tolerance	Features
CNC Milling	Limited by 2.5D / 3-axis machining; tool radius compensation must be considered	± 0.05 - 0.10 mm	High precision; can machine complex surfaces; constrained by tool paths
Laser Cutting	2D only; thickness < 5 mm	± 0.05 - 0.20 mm	Fast; low cost; highly suitable for interlocking assembly structures
3D Printing	Build volume limitations; overhangs may require support	± 0.05 - 0.50 mm	High geometric freedom; supports complex internal cavities and topology; may show layer lines
Molding	Requires molds and draft angles; must be demoldable; may depend on standard part sizes	± 0.01 - 0.50 mm	Relies on master molds or standard libraries; suitable for mass production; inaccessible closed dead cavities are forbidden

Table 2: Material Selection

Material	Compatible Processes	Features
Timber	CNC, Laser Cutting	Easy to process; medium strength; natural texture
PLA-ABS	3D Printing	PLA: easy to print, eco-friendly, low strength; ABS: tough and heat-resistant
Acrylic	CNC, Laser Cutting	Transparent, rigid, but brittle
Resin	3D Printing / Molding	High precision, fine details, brittle
Aluminum	CNC Milling	High strength-to-weight ratio; corrosion-resistant
Steel	CNC Milling	High strength and stiffness; heavy

Table 3: Connection Methods

Joint Type	Features
Interlocking	When properly assembled, it usually constrains all 6 DoFs
Snap-fit	Almost fully constrains motion; relies on elastic deformation
Nailing / Pinning	Partially constrains motion; may allow rotation and axial sliding depending on friction
Pivot / Hinge	Constrains 5 DoF and allows 1 rotational axis
Bonding	Fully constrains motion in all directions; permanent connection

Critical Constraint: Cross-modal Translation Principle

The downstream judge cannot see the source code or the original design document. It can only read your written rubric and inspect '`<Generated_SVG>`' and '`<Reference_SVG>`'.

Therefore, when writing the rubric, you must translate the information in '`<Task_Doc>`' and the background knowledge base into visual inspection instructions that the judge can follow.

Important terminology rule:

- Use **node** only when referring to components in the Component Assembly Graph.
- Use **joint** only when referring to physical connection mechanisms between components.
- Do not use "joint node" or confuse graph nodes with physical joints.
- Normalize joint names before writing the rubric: use **Interlocking** instead of "Mortise & Tenon"; use **Nailing / Pinning** instead of "dowel joint".

Required Rubric Generation Method

You must generate exactly the following six evaluation dimensions.

1. Assembly Readiness

You need to extract '`[Component Assembly Graph (Textual)]`' from '`<Task_Doc>`'.

In the rubric, instruct the judge to infer the Component Assembly Graph from '`<Generated_SVG>`' by treating each visible component as a graph node and each physical connection relationship as an edge. The inferred graph must then be compared with the target graph described in the task.

The Pass criterion must state that the visually inferred node-edge topology is semantically consistent with the target Component Assembly Graph.

The Fail criterion must state that the graph topology is incorrect, such as missing nodes, extra nodes, wrong node-to-node links, disconnected components, or an incorrect central hub.

2. Joint Design

You need to parse '<Task_Doc>' to extract the required joint type and assembly direction. You must also consult Table 3 to obtain the features of that joint type.

In the rubric, the Pass criterion must state that the macroscopic connection location and direction are correct, and that the visual joint design conforms to the required joint type and its physical constraints. You must explicitly mention the features obtained from Table 3, such as whether the joint fully constrains all directions, relies on elastic deformation, or allows a rotational axis.

The Fail criterion must state that the joint design contradicts the specified joint type or its constraint behavior, or that severe rigid-body interpenetration, illegal floating, or physically impossible attachment occurs.

3. Tolerance

You need to extract the manufacturing method from '<Task_Doc>' and consult Table 1 to obtain its precision / tolerance range.

In the rubric, the Pass criterion must explicitly mention the process-level precision value. It must also instruct the judge to use the seam, clearance, wall-thickness, or contact-gap appearance in '<Reference_SVG>' as the visual scale reference. '<Generated_SVG>' should show appropriate independent boundaries, seams, or clearances.

The Fail criterion must state that seams disappear entirely due to illegal fusion, or that the visible gaps are extremely exaggerated and would prevent real-world fitting, slicing, assembly, or functional use.

4. Functional Adaptation

You need to infer 1-2 core functions of the object and clearly separate them into:

- **Must-have function**, usually weighted around 70%.
- **Nice-to-have function**, usually weighted around 30%.

In the rubric, the Pass criterion must state that the visual proportions and structures fully satisfy the must-have function and include the basic structures needed for the nice-to-have function.

The Fail criterion must give concrete fatal-error examples, such as the must-have function being completely lost, or the nice-to-have feature becoming extremely distorted and damaging the overall must-have use.

5. Usage Stability

You need to extract the intended stability, anti-tipping, load-bearing, or support behavior from '<Task_Doc>', and infer the force-transfer path based on the component topology and physical joints.

In the rubric, the Pass criterion must state that '<Generated_SVG>' shows a stable support posture, reasonable load transfer, and load-bearing members with safe visual thickness.

The Fail criterion must list cases that would inevitably cause tipping, collapse, or structural instability, such as centered support points, uneven legs, extremely thin load-bearing members, insufficient base contact, or disconnected load paths.

6. Manufacturability

You need to extract '[Material]' and '[Manufacturing Method]' from '<Task_Doc>'. You must cross-check Table 1 and Table 2 to verify the process constraints and material features.

In the rubric, the Pass criterion must state that '<Generated_SVG>' uses conventional geometries compatible with the specified process and the physical features of the material.

The Fail criterion must list topology or geometry features that violate the process or material constraints, such as inaccessible internal dead cavities for CNC machining, zero-thickness surfaces, non-manifold geometry for 3D printing, or extremely thin load-bearing cantilevers made from brittle materials.

Input Modalities

Only you can see the following inputs. Do not reveal source code or raw design documents to the downstream judge.

1. '<Task_Doc>': the design specification, including design goals, component list, parameter ranges, and assembly graph.
2. '<Reference_Code>': the ground-truth CAD logic and spatial coordinates.
3. '<Reference_SVG>': the visual anchor / reference image.

Output Template

Strictly follow the Markdown template below.

You must use the exact terms '<Reference_SVG>' and '<Generated_SVG>' in the rubric.

Write the instructions as if you are directly guiding the downstream judge.

Do not include a separate "Core Focus" field. Instead, merge all necessary inspection guidance into the Pass criterion.

1. Assembly Readiness

* **Evaluation Rubric (0-1 Score)**:

* **1 Point (Pass)**: [Instruct the judge to infer the Component Assembly Graph from '<Generated_SVG>'; describe the required target graph using node-edge language; state what counts as a correct visual topology.]

* **0 Points (Fail)**: [Describe incorrect graph topology, such as missing nodes, extra nodes, incorrect links, disconnected components, or wrong hub structure.]

2. Joint Design

* **Evaluation Rubric (0-1 Score)**:

* **1 Point (Pass)**: [Describe the required joint type, physical constraint behavior, connection location, assembly direction, and acceptable visual appearance.]

* **0 Points (Fail)**: [Describe joint-type mismatch, wrong direction, missing attachment, illegal floating, severe interpenetration, or physically impossible connection.]

3. Tolerance

* **Evaluation Rubric (0-1 Score)**:

* **1 Point (Pass)**: [Mention the manufacturing precision value; instruct the judge to use '<Reference_SVG>' as the visual scale reference; describe acceptable seams, clearances, wall thickness, or contact gaps.]

* **0 Points (Fail)**: [Describe illegal fusion, exaggerated gaps, missing clearances, invalid wall thickness, or tolerance errors that make the object impossible to assemble, slice, or use.]

4. Functional Adaptation

* **Evaluation Rubric (0-1 Score)**:

* **1 Point (Pass)**: [State the must-have function and nice-to-have function; describe how '<Generated_SVG>' visually satisfies them.]

* **0 Points (Fail)**: [Give concrete fatal examples where the must-have function is lost, or the nice-to-have feature severely damages the must-have use.]

5. Usage Stability

* **Evaluation Rubric (0-1 Score)**:

* **1 Point (Pass)**: [Describe the intended support / load-transfer / anti-tipping behavior; specify what stable visual geometry should look like.]

* **0 Points (Fail)**: [Describe inevitable tipping, collapse, deformation, unstable support, missing support points, or broken load paths.]

6. Manufacturability

* **Evaluation Rubric (0-1 Score)**:

* **1 Point (Pass)**: [State the material and manufacturing process; describe geometries compatible with the process and material.]

* **0 Points (Fail)**: [Describe geometry or topology that violates material/process constraints, such as zero-thickness surfaces, inaccessible cavities, non-manifold geometry, impossible overhangs, or physically fragile structures.]

Few-shot Reference

Example 1: Four-legged Dining Chair with Backrest

1. Assembly Readiness

* **Evaluation Rubric (0-1 Score)**:

* **1 Point (Pass)**: Ask the judge to infer the Component Assembly Graph from '<Generated_SVG>' by treating each visible component as a graph node and each physical connection relationship as an edge. The inferred graph must match the target topology: 'seat_panel' is the only central hub node; 'front_left_leg', 'front_right_leg', 'rear_left_leg', and 'rear_right_leg' each connect to the four lower corners of 'seat_panel'; 'backrest_panel' connects to the rear side of 'seat_panel'. The object should be visually identifiable as a 6-component dining chair consisting of 1 seat panel, 4 legs, and 1 backrest.

* **0 Points (Fail)**: The graph topology is incorrect. For example, the backrest is floating instead of connected to the seat panel; a leg is connected to the backrest or to another leg instead of the seat panel; any leg is missing; extra components such as armrests or crossbars alter the required 6-component structure; or the seat panel is no longer the central hub node.

2. Joint Design

* **Evaluation Rubric (0-1 Score)**:

* **1 Point (Pass)**: Ask the judge to inspect the assembly regions shown in '<Reference_SVG>' and verify that the macroscopic connection locations and assembly directions in '<Generated_SVG>' are correct. The four legs should insert upward along the +Z direction into sockets on the underside of the seat panel, and the backrest should press downward along the -Z direction into the long rear slot of the seat panel. The required joint is Interlocking: when properly assembled, it usually constrains all 6 degrees of freedom. Visually, the leg protrusions should appear to enter the seat sockets, and the backrest strip should appear to enter the rear slot with tight engagement. Minor line overlap caused by SVG rendering or projection is acceptable.

* **0 Points (Fail)**: The joint design contradicts the Interlocking behavior. For example, the legs merely touch the outer sides of the seat without an insertion relationship; the backrest floats above the seat; the slot or insertion direction is wrong; severe interpenetration occurs between rigid bodies; or the connection points are so misaligned that the protrusions could not enter the corresponding sockets or constrain all 6 degrees of freedom.

3. Tolerance

* **Evaluation Rubric (0-1 Score)**:

* **1 Point (Pass)**: The manufacturing process is CNC Milling, whose expected precision is ± 0.05 -0.10 mm. Ask the judge to use the thin

visual seams and interlocking contact boundaries in '<Reference_SVG>' as the scale reference. In '<Generated_SVG>', the boundaries between the seat panel and legs, and between the seat panel and backrest, should remain visible as very fine seams or tight contact lines. The fit should visually suggest a CNC-machined tight interlocking assembly: the clearance is small, but the component boundaries do not disappear.

* **0 Points (Fail)**: The seams disappear completely, making the seat, legs, and backrest look illegally fused into a single body; or the visible gaps are extremely exaggerated, such as legs visibly separated from the seat or a large gap between the backrest and the rear slot, making real interlocking fitting or load transfer impossible.

4. Functional Adaptation

* **Evaluation Rubric (0-1 Score)**:

* **1 Point (Pass)**: The must-have function, weighted around 70%, is to serve as a single-person dining chair that supports human body weight and provides a reasonable seat width, depth, and height. The nice-to-have function, weighted around 30%, is to provide basic back or lumbar support through the backrest. In '<Generated_SVG>', the seat should have a reasonable square or rectangular sitting surface, the four legs should support it at a plausible chair height, and the backrest should be positioned behind the seat with sufficient height to provide support. The whole object should be recognizable as a usable four-legged dining chair rather than an abstract frame or decorative object.

* **0 Points (Fail)**: The must-have function is completely lost. For example, the seat is extremely narrow or paper-thin and cannot visually support a person; the legs are so short or tall that the seat height is unusable; the backrest appears at the front or side of the chair or is missing; or the backrest is extremely distorted, heavily tilted, or passes through the center of the seat in a way that destroys the sitting function.

5. Usage Stability

* **Evaluation Rubric (0-1 Score)**:

* **1 Point (Pass)**: Ask the judge to evaluate anti-tipping posture, support polygon size, and the visual load-transfer path. The intended force path is: human weight → 'seat_panel' → four corner legs → ground. '<Generated_SVG>' should resemble '<Reference_SVG>' by showing four vertical legs distributed near the seat edges or corners, with consistent leg length so the seat can remain level. The legs and seat panel should have safe visual thickness. The center of gravity should plausibly fall inside the support region formed by the four legs. Although the backrest introduces rearward torque, it should be stabilized through the rear legs and the interlocking connection to the seat panel.

* **0 Points (Fail)**: The object would inevitably tip or fail structurally. For example, the four legs are clustered near the center, producing a tiny support polygon; only two or three legs touch the ground; leg lengths are inconsistent; the rear legs are missing while the backrest is tall, causing backward tipping; or the legs or seat are visually as thin as lines and cannot support a seated person.

6. Manufacturability

* **Evaluation Rubric (0-1 Score)**:

* **1 Point (Pass)**: The material is Timber and the manufacturing process is CNC Milling. Timber is compatible with CNC machining, easy to process, medium strength, and has natural texture. CNC Milling has ± 0.05 - 0.10 mm precision but is constrained by 2.5D / 3-axis tool paths and tool radius. '<Generated_SVG>' should use conventional wood-CNC geometries: a rectangular seat panel, four square-post legs, a vertical backrest panel, and understandable rectangular interlocking interfaces. The components should remain visually distinguishable as independent closed solids, and the original 6-component split should not be altered.

* **0 Points (Fail)**: '<Generated_SVG>' shows geometry or topology that violates Timber or CNC Milling constraints. Examples include zero-thickness seat or backrest surfaces, inaccessible internal dead cavities that a CNC tool cannot reach, extremely thin load-bearing wooden cantilevers or needle-like legs, margins so small that wood splitting is visually likely, illegal fusion of multiple components into an inseparable body, or overly organic surfaces that cannot reasonably be produced by conventional 3-axis wood CNC machining.

Example 2: Wave Vase

1. Assembly Readiness

* **Evaluation Rubric (0-1 Score)**:

* **1 Point (Pass)**: Ask the judge to infer the Component Assembly Graph from '<Generated_SVG>'. The target graph is 'wave_vase_body -> Standalone', with Joint: None. The inferred topology must match this target: the model should contain exactly one standalone graph node, 'wave_vase_body', with no extra components, no separated parts, and no movable joints. The outer shell, inner cavity, base, and top rim should all belong to the same continuous vase body.

* **0 Points (Fail)**: The graph topology is incorrect. For example, the model is split into multiple separated petal-like panels; the outer shell and inner liner appear as two independent components; the base is detached from the body; extra components such as handles, stands, or lids appear; or the object looks like an assembly of multiple parts rather than one standalone body.

2. Joint Design

* **Evaluation Rubric (0-1 Score)**:

* **1 Point (Pass)**: The required joint type is N/A because this is a single continuous body with no physical assembly joint, no hinge, no bonding, no snap-fit, and no interlocking interface. '<Generated_SVG>' should appear as one continuous and complete vase. The outer wall, inner wall, top rim, and base should visually connect naturally without separated parts or assembly seams. Since Joint is None, screws, hinges, snap features, glue pads, slots, and protrusions should not appear. Minor triangular mesh texture or shading transitions caused by curved-surface rendering are acceptable.

* **0 Points (Fail)**: The connection semantics contradict the task. For example, the vase is divided into multiple pieces that would need bonding or insertion; the top rim is detached from the body; the inner wall floats like a separate cup liner; the base is separated from the outer shell; or non-required joint features such as hinges, snap-fits, screw holes, or slots appear.

3. Tolerance

* **Evaluation Rubric (0-1 Score)**:

* **1 Point (Pass)**: The manufacturing process is FDM Printing, treated under the 3D Printing precision range of ± 0.05 -0.50 mm. Because this is not an assembly model, the tolerance check should focus on printable wall thickness, top rim thickness, the spacing between inner and outer walls, and bottom closure thickness rather than part-to-part fitting. Ask the judge to use the visible wall thickness at the top opening and the solid base appearance in '<Reference_SVG>' as the visual scale reference. '<Generated_SVG>' should show a clear hollow opening, an identifiable thick-wall structure, and a continuous rim. The wall should not be nearly zero-thickness, and it should not be so thick that the opening is almost blocked. Slight layer lines, mesh artifacts, or surface discretization are acceptable for FDM-style output.

* **0 Points (Fail)**: The wall-thickness or opening tolerance is severely wrong. For example, the top opening disappears and the object becomes a solid sculpture; the inner and outer wall boundaries are visually chaotic and the cavity cannot be identified; the wall is paper-thin and likely to break under FDM printing; the wall thickness is so exaggerated that the opening becomes unusably narrow or the body becomes bulky; or the bottom is not closed, making the object invalid as a container or as a slicable closed body.

4. Functional Adaptation

* **Evaluation Rubric (0-1 Score)**:

* **1 Point (Pass)**: The must-have function, weighted around 70%, is to serve as a desktop decorative vase with a stable solid base, a clear hollow container form, and a top opening, at least suitable for display or holding lightweight dried flowers. The nice-to-have function, weighted around 30%, is the twisted corrugated aesthetic. '<Generated_SVG>' should clearly appear as a vase that can stand on a desk: it should have a stable bottom, an expanding or contracting decorative body profile, a visible top opening and rim, and an interior cavity. The outer wall should show continuous twisting waves or vertical corrugations, and the aesthetic deformation must not destroy the container function.

* **0 Points (Fail)**: The must-have function is completely lost. For example, the model is a solid block with no opening; there is no flat base or the bottom is pointed so it cannot stand; the top is sealed and cannot hold dried flowers; the form collapses, self-intersects, or breaks so badly that it is no longer recognizable as a vase; or the waves are so extreme that the body is torn, punctured, or twisted into an unusable abstract sculpture.

5. Usage Stability

* **Evaluation Rubric (0-1 Score)**:

* **1 Point (Pass)**: Ask the judge to evaluate desktop standing stability, base support area, center-of-mass position, and safe wall thickness. The vase is non-load-bearing but should support its own weight and a small amount of lightweight dried flowers. The intended force path is: vase self-weight / dried flowers → thick shell and base → tabletop. '<Generated_SVG>' should resemble '<Reference_SVG>' by having a solid flat or near-flat base with sufficient contact area, and the body's center of mass should remain roughly near the central vertical axis. The wave pattern should be distributed evenly enough that the vase does not visibly lean to one side. The wall thickness should appear sufficient for FDM-printed shell stiffness, and the top rim should not be too thin or broken.

* **0 Points (Fail)**: The object would inevitably tip or fail structurally. For example, the bottom is a sharp point or has an extremely small contact area; the body bulges heavily to one side so the center of mass falls outside the base; the vase is extremely tall and narrow with an insufficient base; the wall is paper-thin and the rim is broken; or the base is missing or perforated so it cannot stand stably.

6. Manufacturability

* **Evaluation Rubric (0-1 Score)**:

* **1 Point (Pass)**: The material is PLA and the manufacturing process is FDM Printing. PLA is easy to print but relatively low-strength, while FDM / 3D Printing supports complex geometry but requires a slicable closed manifold solid. Very thin walls, non-manifold edges, self-intersecting surfaces, and uncontrolled overhangs may cause print failure. '<Generated_SVG>' should show a single thick-wall body compatible with PLA/FDM printing: a continuous outer shell, a clear hollow interior, a closed base, a continuous top rim, and no obvious non-manifold cracks. The twisted waves may be complex, but they should remain smooth, continuous, non-self-intersecting, and free of unexplained floating surfaces or internal fragments.

* **0 Points (Fail)**: '<Generated_SVG>' violates FDM / PLA manufacturing constraints. For example, it is not a single closed manifold body; the outer shell has large cracks or self-intersections; isolated surfaces float inside the cavity; the bottom is not closed; the wall is nearly zero-thickness; the top rim breaks into multiple independent pieces; or the design contains extremely thin, long-span suspended PLA structures that would collapse or snap during printing.

Now wait for the user to provide '<Task_Doc>', '<Reference_Code>', and '<Reference_SVG>', then dynamically generate the task-specific rubric.
""

Table 9: Per-model results across the three evaluation stages, judged by *GPT-5.5*. The table reports code execution, geometric validity, and design-intent alignment scores under our funnel-style evaluation protocol. Bold marks the best score per block.

Model	Code Check (%)		Geometry Check (%)				Design Intent Alignment (%)			
	Sandbox Success	Watertight	Manifold	Self-Int. Free	Overlap Free	Geom. Valid	Functionality	Manufacturability	Assemblability	Final Score
<i>Closed-Source Models</i>										
claude-opus-4.7	76.42	76.42	76.42	73.58	60.38	58.49	53.77	54.72	51.89	53.46
claude-3.7-sonnet	46.23	46.23	46.23	46.23	23.58	23.58	17.45	19.34	16.98	17.92
gemini-3.1-pro	65.09	59.43	63.21	63.21	62.26	58.49	53.77	55.19	52.83	53.93
glm-5.1	31.13	31.13	31.13	31.13	27.36	27.36	22.64	25.00	24.53	24.06
glm-4.7-flash	8.49	7.55	7.55	7.55	5.66	5.66	2.83	2.83	2.83	2.83
gpt-5.5	77.36	72.64	74.53	73.58	70.75	68.87	66.51	66.98	67.92	67.14
gpt-4o	36.79	36.79	36.79	36.79	13.21	13.21	8.02	9.91	8.49	8.81
minimax-m2.7	18.87	18.87	18.87	18.87	10.38	10.38	8.02	8.49	8.02	8.18
minimax-m2.5	25.47	22.64	22.64	22.64	10.38	10.38	4.72	6.60	4.72	5.35
<i>Average</i>	42.87	41.30	41.93	41.51	31.55	30.71	26.42	27.67	26.47	26.85
<i>Open-Source Models</i>										
qwen-3.5-122b-a10b	27.36	25.47	25.47	25.47	13.21	13.21	10.38	10.38	10.38	10.38
qwen-2.5-72b	50.00	49.06	49.06	49.06	19.81	20.75	8.02	14.15	8.96	10.38
llama-3.1-70b	31.13	30.19	30.19	30.19	22.64	23.58	3.77	8.96	3.77	5.50
qwen-3.6-35b-a3b	8.49	8.49	8.49	8.49	5.66	5.66	4.72	4.72	4.72	4.72
qwen-3.6-coder	14.15	14.15	14.15	14.15	10.38	10.38	4.72	6.13	5.19	5.35
llama-3.1-8b	2.83	1.89	1.89	1.89	0.94	1.89	0.00	0.00	0.00	0.00
<i>Average</i>	22.33	21.54	21.54	21.54	12.11	12.58	5.27	7.39	5.50	6.05

Table 10: Stage 3 sub-criterion breakdown judged by *GPT-5.5*; *Average* is the mean of the two sub-criterion columns to its left. Bold marks the best score per block.

Model	Functionality (%)			Manufacturability (%)			Assemblability (%)		
	Functional	Robust	<i>Average</i>	Well-toleranced	Manufacturable	<i>Average</i>	Assembly-ready	Connectable	<i>Average</i>
<i>Closed-Source Models</i>									
claude-opus-4.7	52.83	54.72	53.77	53.77	55.66	54.72	52.83	50.94	51.89
claude-3.7-sonnet	16.04	18.87	17.45	17.92	20.75	19.34	16.98	16.98	16.98
gemini-3.1-pro	52.83	54.72	53.77	53.77	56.60	55.19	53.77	51.89	52.83
glm-5.1	21.70	23.58	22.64	23.58	26.42	25.00	24.53	24.53	24.53
glm-4.7-flash	2.83	2.83	2.83	2.83	2.83	2.83	2.83	2.83	2.83
gpt-5.5	65.09	67.92	66.51	66.98	66.98	66.98	67.92	67.92	67.92
gpt-4o	7.55	8.49	8.02	7.55	12.26	9.91	8.49	8.49	8.49
minimax-m2.7	7.55	8.49	8.02	8.49	8.49	8.49	9.43	6.60	8.02
minimax-m2.5	4.72	4.72	4.72	5.66	7.55	6.60	4.72	4.72	4.72
<i>Average</i>	25.68	27.15	26.42	26.73	28.62	27.67	26.83	26.10	26.47
<i>Open-Source Models</i>									
qwen-3.5-122b-a10b	9.43	11.32	10.38	8.49	12.26	10.38	10.38	10.38	10.38
qwen-2.5-72b	7.55	8.49	8.02	9.43	18.87	14.15	9.43	8.49	8.96
llama-3.1-70b	2.83	4.72	3.77	4.72	13.21	8.96	3.77	3.77	3.77
qwen-3.6-35b-a3b	4.72	4.72	4.72	4.72	4.72	4.72	4.72	4.72	4.72
qwen-3.6-coder	4.72	4.72	4.72	4.72	7.55	6.13	5.66	4.72	5.19
llama-3.1-8b	0.00	0.00	0.00	0.00	0.00	0.00	0.00	0.00	0.00
<i>Average</i>	4.87	5.66	5.27	5.35	9.43	7.39	5.66	5.35	5.50

Table 11: Same correlations as Table 4 with 95% bootstrap confidence intervals (in brackets).

Level	Gemini 3.1 Pro			GPT-5.5			GPT-4o		
	Pearson r	Spearman ρ	Kendall τ	Pearson r	Spearman ρ	Kendall τ	Pearson r	Spearman ρ	Kendall τ
Sub-criteria	0.713 [0.668, 0.757]	0.705 [0.659, 0.751]	0.655 [0.611, 0.698]	0.659 [0.609, 0.708]	0.653 [0.603, 0.701]	0.607 [0.559, 0.653]	0.620 [0.561, 0.676]	0.609 [0.550, 0.664]	0.566 [0.509, 0.618]
Criteria	0.762 [0.706, 0.815]	0.749 [0.689, 0.804]	0.668 [0.610, 0.723]	0.712 [0.648, 0.774]	0.705 [0.639, 0.764]	0.626 [0.565, 0.685]	0.703 [0.637, 0.769]	0.685 [0.615, 0.752]	0.610 [0.544, 0.674]
Design instance	0.835 [0.770, 0.893]	0.831 [0.756, 0.880]	0.694 [0.610, 0.767]	0.775 [0.679, 0.859]	0.773 [0.674, 0.844]	0.654 [0.566, 0.730]	0.826 [0.769, 0.876]	0.799 [0.723, 0.854]	0.663 [0.582, 0.735]